Current Applied Physics 12 (2012) 188–192

Contents lists available at ScienceDirect

Current Applied Physics

journal homepage: www.elsevier.com/locate/cap

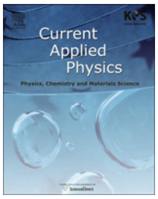

Preparation and thermoelectric properties of $AgPb_{18}SbTe_{20-x}Se_x$ ($x = 1, 2, 4$) materials

H. Li [a], K.F. Cai [a,*], Y. Du [a,b], H.F. Wang [a], S.Z. Shen [b], X.L. Li [a], Y.Y. Wang [a], C.W. Zhou [a]

[a] Functional Materials Research Laboratory, Tongji University, 1239 Siping Road, Shanghai 200092, China
[b] CSIRO Materials and Engineering Division, 37 Graham Road, Highett, VIC 3149, Australia

ARTICLE INFO

Article history:
Received 22 June 2010
Received in revised form
26 May 2011
Accepted 27 May 2011
Available online 22 June 2011

Keywords:
PbTe
Hydrothermal synthesis
Thermoelectric property

ABSTRACT

$AgPb_{18}SbTe_{20-x}Se_x$ ($x = 1, 2, 4$) bulk materials were prepared by combining hydrothermal synthesis and melting. Thermoelectric properties were measured from room temperature up to 773K. The materials showed n-type conduction and exhibited degenerate semiconductor behavior. The power factors of the materials varied greatly with increase of Se content (x). Partial substitution of Se for Te in $AgPb_{18}SbTe_{20}$ resulted in remarkable reduction of thermal conductivity in the whole temperature range and increase of power factor at lower temperatures; therefore, the dimensionless figure of merit, ZT, was enhanced below 600K. A maximum ZT value of ~0.82 is obtained at 523K for the $AgPb_{18}SbTe_{18}Se_2$ sample.

1. Introduction

With the world's increasing demand for energy and the environmental problem becoming more and more serious, thermoelectric (TE) materials have recently attracted increasing attention due to their promising applications in TE power generation or cooling [1–3]. The efficiency of a TE device depends on the TE properties of the materials used. Whereas the effectiveness of a TE material is determined by its dimensionless figure of merit, $ZT = S^2\sigma T/\kappa$, where T is the absolute temperature, S is the Seebeck coefficient, σ is the electrical conductivity and κ is the thermal conductivity of the material. A good TE material requires high electrical conductivity, high Seebeck coefficient and at the same time low thermal conductivity. However, it is generally very difficult to simultaneously achieve increased $S^2\sigma$ and reduced κ because of the interdependence of the three parameters [4].

Persistent efforts have been made on enhancing the ZT values of TE materials [2,4,5]. Doping and alloying have been demonstrated as effective ways to improve TE properties, but it is still not easy to obtain TE materials with $ZT > 1$ [6–8]. Significant enhancement in ZT values were reported for superlattices of Bi_2Te_3/Sb_2Te_3 [9] and $PbSe_{0.98}Te_{0.02}/PbTe$ [10] because of markedly reduction in the lattice thermal conductivity. However, it is difficult to use these superlattices in large-scale applications because of limitations in both heat transfer and cost [11]. Recently, bulk TE materials composed of nanometer-size grains [11,12] or with other nanometer-scale internal structures (nanoclusters) [13–16] have exhibited enhanced ZT values. For example, Kanatzidis and coworkers [13] reported that the Ag and Sb co-doped PbTe, $AgPb_mSbTe_{2+m}$, or LAST-m (LAST stands for Lead Antimony Silver Tellurium) materials, prepared by melting high-purity elemental Ag, Pb, Sb and Te at 1123K for 4 h followed by a slow cooling, have extremely high ZT values ($ZT = 1.7$ at 700K for LAST-18). LAST-m system materials have recently attracted much attention and have been prepared by other methods such as hot pressing [17], mechanical alloying combined with spark plasma sintering [18,19]. In addition, other interrelated materials such as $Na_{1-x}Pb_mSb_yTe_{2+m}$ [20], $Ag(Pb_{1-y}Sn_y)_mSbTe_{2+m}$ [21], and $Ag_{1-x}Pb_{18}(Sb,Bi)Te_{20}$ [22] were successively reported by the Kanatzidis group. Similar to the LAST-m materials, these bulk materials also contain nanoclusters and have enhanced ZT values. However, not all the LAST-18 materials contain nanoclusters. For example, Zhu et al. [23] reported homogenous $AgPb_{18}Sb_{1-x}Te_{20}$ bulk compounds prepared by quenching the melts of high-purity elemental Ag, Pb, Sb and Te in liquid nitrogen.

We have developed a cost-effective route to the LAST-m materials by combining hydrothermal synthesis and melting. The obtained LAST-18 material shows a highest ZT value of 0.94 at 723K [24]. This value is lower than that reported in Refs. [13,19], mainly due to the material with higher thermal conductivity. It has been

---

* Corresponding author. Tel./fax: +86 21 65980255.
E-mail address: kfcai@tongji.edu.cn (K.F. Cai).

1567-1739/$ – see front matter © 2011 Elsevier B.V. All rights reserved.
doi:10.1016/j.cap.2011.05.035

reported that partial substitution of Se for Te in PbTe [25] and also in $Pb_{9.6}Sb_{0.2}Te_{10}$ [14] can significantly reduce thermal conductivity. Herein we investigate the TE properties of $AgPb_{18}SbTe_{20-x}Se_x$ ($x = 1, 2, 4$) materials which were prepared by the same method as described in Ref. [24].

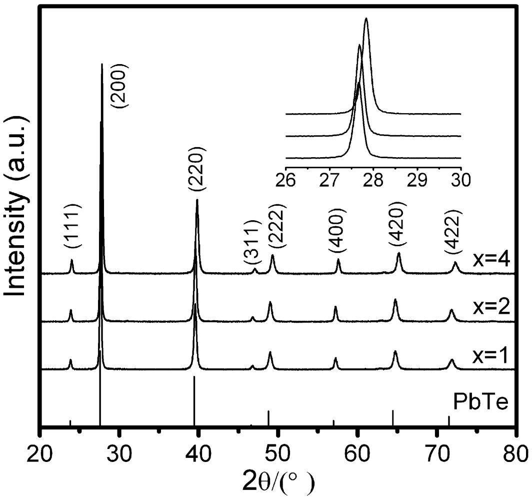

Fig. 1. XRD patterns of $AgPb_{18}SbTe_{20-x}Se_x$ ($x = 1, 2, 4$) bulk materials. The inset is an expanded pattern between $2\theta = 26–30°$.

2. Experimental procedure

Analytical purity $AgNO_3$, $Pb(NO_3)_2$, $SbCl_3$, TeO_2, and Se powder were used as the starting materials. $AgPb_{18}SbTe_{20-x}Se_x$ ($x = 1, 2, 4$) powders were prepared by varying the molar ratio of $AgNO_3$, $Pb(NO_3)_2$, $SbCl_3$, TeO_2, and Se. As an example, the preparation of $AgPb_{18}SbTe_{19}Se$ powder was described as follows. About 40 mL deionized water was poured into a 100-mL beaker, and the beaker was placed on the plate of a magnetic force stirring device. The $AgNO_3$ (0.23 mmol), $Pb(NO_3)_2$ (4.13 mmol), $SbCl_3$ (0.23 mmol), TeO_2 (4.36 mmol), and Se powder (0.23 mmol) were added into the beaker one by one with constant stirring by a magnetic bar; after that, KOH (0.12 mol) and KBH_4 (0.035 mol) were added into the beaker. The mixture was kept under stirring for 10 min before being poured into a 100-mL teflon autoclave. Some deionized water was added into the autoclave until ~85% of its volume was filled. The autoclave was sealed and then put into an oven. The oven was heated up to 180 °C and held at 180 °C for 20 h, and finally cooled naturally to room temperature. Black precipitates were collected and washed with deionized water and absolute ethanol in sequence for several times, and then separated by centrifugation for 5 min at 4000 rpm. The obtained black powders were dried in vacuum at 70 °C for 6 h. The dried powders were loaded into a BN-lined graphite crucible and then sealed in a quartz tube under 6.7×10^{-3} Pa before being flushed with argon for several times. The quartz tube was heated to 1173–1373K, held at the temperature for 5 h, and then cooled to 723 K in 60 h, followed by naturally cooling to room temperature. Cylinder-like ingot was obtained at the bottom of the graphite crucible.

The phase composition of the bulk samples was examined by X-ray diffraction (XRD, Rigaku D/max2550), with Cu K_α radiation (λ = 1.5406 Å). Room temperature optical diffuse reflectance measurements were performed on powders ground from the bulk samples, using a Nicolet NEXUS870 FT-IR spectrometer. The infrared absorption spectra were monitored in the region of 400–4000 cm^{-1}. Absorption data were calculated from reflectance data using the Kubelka–Munk function. The band gaps were determined as the intersection point between energy axis at the absorption offset and the line extrapolated from the linear absorption edge in a α/S_c (where α is absorption coefficient, S_c is the scattering coefficient) versus energy plots. Scanning electron microscopy (SEM, JEOL JSM5510) was used to observe the fracture surface of the bulk samples. And the fracture surfaces after grinding and polishing were examined by field emission SEM (FESEM, Quanta 200 FEG) equipped with energy dispersive X-ray spectrometry. The bulk samples were cut into pellets (~1 mm in thickness and 10 mm in diameter) and rectangular pieces ($10 \times 1 \times 2$ mm^3) for thermal and electrical properties measurement, respectively. Electrical conductivity measurement was performed using a steady-state four-probe technique with a square wave current (~10 mA in amplitude), and the Seebeck coefficient was determined by the slope of the linear relationship between the thermoelectromotive force and temperature difference (~10 K) between the two ends of each sample. The Hall coefficient and carrier concentration of the samples were measured at room temperature using HMS-3000 (Ecopia) with a magnetic field of 0.55 T. Thermal conductivity (κ) was calculated using the equation $\kappa = \upsilon C_p d$, where υ is the thermal diffusivity, C_p is the specific heat, and d is density of the samples. The thermal diffusivity was measured from ~300–723K on a laser flash apparatus (Netzsch, LFA-457) in Ar, and the specific heat was measured using differential scanning calorimeter (Netzsch, DSC 404) in Ar. The bulk density was determined by the Archimedes method.

3. Results and discussion

Fig. 1 shows the XRD patterns of the bulk $AgPb_{18}SbTe_{20-x}Se_x$ ($x = 1, 2, 4$) materials. The XRD patterns indicate that all the samples are single phase with NaCl-type structure ($Fm\overline{3}m$) and have almost the same XRD pattern as that for PbTe (JCPDS Card file,

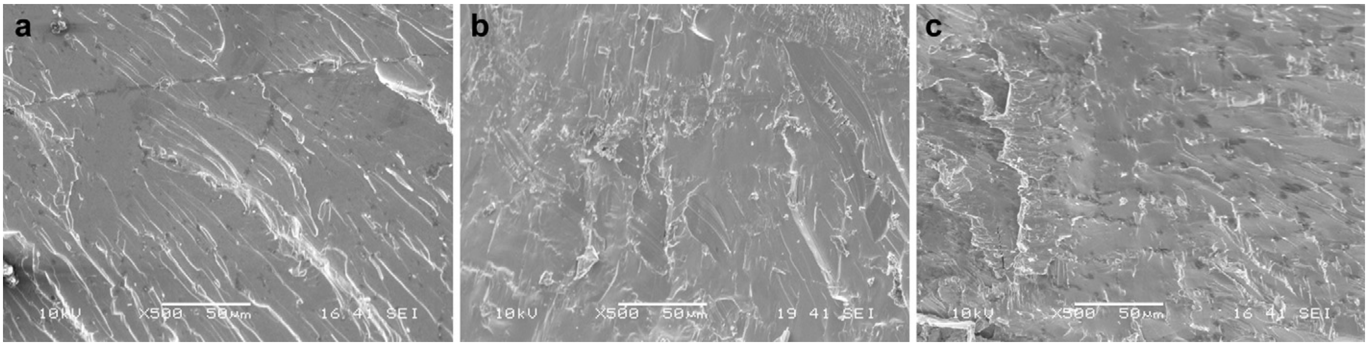

Fig. 2. SEM images of the fracture surfaces of the $AgPb_{18}SbTe_{19}Se$ (a), $AgPb_{18}SbTe_{18}Se_2$ (b), and $AgPb_{18}SbTe_{16}Se_4$ (c) materials, respectively. The bars denote 50 μm.